Bioconjugate Chemistry

Article

Cite This: *Bioconjugate Chem.* 2019, 30, 218−230

pubs.acs.org/bc

Matrix-Assisted Regulation of Antimicrobial Properties: Mechanistic Elucidation with Ciprofloxacin-Based Polymeric Hydrogel Against *Vibrio* Species

Ishita Mukherjee,[†] Anwesha Ghosh,[‡] Punyasloke Bhadury,[*,‡,§] and Priyadarsi De[*,†,§]

[†]Polymer Research Centre, Department of Chemical Sciences, [‡]Integrative Taxonomy and Microbial Ecology Research Group, Department of Biological Sciences, [§]Centre for Advanced Functional Materials, Indian Institute of Science Education and Research Kolkata, Mohanpur, Nadia, West Bengal 741246, India

Supporting Information

ABSTRACT: The design of a new drug material through modification of some well-known antibiotics to combat pathogenic bacteria must include a complete understanding of matrix regulation because the human body consists of primarily three types of matrices, that is, solid, semisolid, and liquid, all of which have a tendency to regulate antibacterial efficacy along with the bactericidal mechanism of several antimicrobial agents. Herein, matrix-dependent action of ciprofloxacin-based polymeric hydrogel scaffold was explored against a new species of *Vibrio*, namely, *Vibrio chemaguriensis* Iso1 (*V. chemaguriensis*), which is resistant to most of the common antibiotics and possess genes that can be linked to pathogenicity. Ciprofloxacin was attached to the polymeric system consisting of hydrophilic polyethylene glycol methyl ether methacrylate (PEGMA) and zwitterionic sulphabetaine methacrylate (SBMA) with an antifouling nature via covalent linkage leading to effective polymer antibiotic conjugates (PACs) with linear and hyperbranched architectures. The hyperbranched PAC was transformed to a polymeric gel exhibiting greater antibacterial efficacy in solid matrix than that of the liquid one with a complete bactericidal effect and rod to spherical switching of bacterial cell followed by chain formation via "dual" contact activity and release mechanism through sustained removal of thiol-terminated ciprofloxacin fragment along with an equilibrium swelling and deswelling process. Lower killing efficacy was displayed in the liquid matrix with an intact cell morphology that is due to lack of forced contact between the cell wall and gel surface as well as entrapment of released bioactive fragment via an additional thick exopolysaccharide (EPS) layer, which represents a great challenge to modern medical sciences.

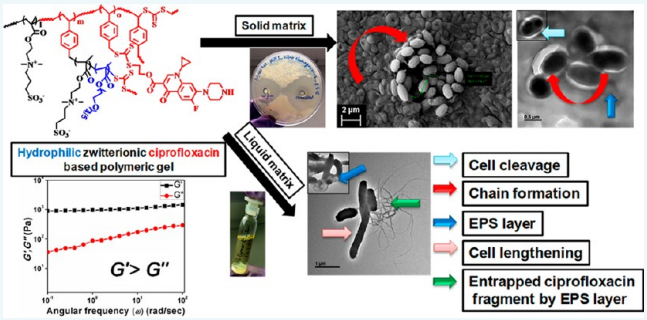

INTRODUCTION

The recent development of numerous drug-resistant pathogenic bacteria is caused by excessive use of conventional antibiotics for treatment purposes.[1,2] Sometimes, the limited penetration of antibiotics into the target sites result in rampant nosocomial infections including infections in vascular (e.g., bone), avascular (e.g., cartilage), or necrotic tissues (e.g., surgical incisions, SSI).[3,4] Surgical cases are further complicated by microbial biofilm formation under postoperation scenarios.[5] Of every 100 hospitalized patients, 7 in developed and 10 in developing countries can acquire nosocomial infections.

High costs for new drug development and stringent approval protocols result in fewer trials of new antimicrobial agents per year.[6,7] An alternative path to shorten the time of development for new antimicrobial agents is formulation and derivatization of existing antibiotics with modified functional groups or alteration of charge density, solubility, degradability, selectivity, and efficiency.[8,9] Target specificity of these drugs can be further enhanced by molecular modifications with liposomes, micelles, or nanomaterials.[10,11] Efficient derivatization of antibiotics with polymeric material could be a promising alternative for a new class of antibiotics because of the lower toxicity, increased solubility, and prolonged activity originating from polymer antibiotic conjugates (PACs).[12,13] Although there are several reports regarding the potential applications of PACs in detoxification of anticancer drugs such as doxorubicin,[14,15] in therapeutic antibiotic carriers by using degradable[16,17] or nondegradable[18,19] polymer matrices, ittle attention has been paid toward exploring permanently bound polymer antibiotic conjugates on the treatment of bacterial infections.[20] Introduction of commonly employed polyethylene glycol to several antibiotics moieties like penicillin V,[21] tobramycin[22] or vancomycin[23] can lead to generation of a series of PACs which could exhibit antimicrobial properties against several microorganisms including bacteria. Polyacrylates[24] and poly(*N*-isopropylacrylamide) (PNIPAM)[25] have also been used to generate antibacterial PACs. Continuous

Received: November 22, 2018
Revised: December 4, 2018
Published: December 5, 2018

DOI: 10.1021/acs.bioconjchem.8b00846
Bioconjugate Chem. 2019, 30, 218−230

efforts to enhance the antibacterial efficiency of PACs toward infection-causing bacteria would become mandatory to combat the increasing cases of antidrug resistance in the future world.

On the other hand, a porous, moist, and robust structure of highly cross-linked three-dimensional (3D) hydrogel matrix may lead to enhanced drug delivery and reduced biofilm formation.[26] The broad-spectrum activity of gel network originates from their structural integrity. Several hydrogel systems generated from natural or synthetic polymers including chitosan-iron oxide coated graphene oxide nanocomposite hydrogel,[27] cationic chitosan- or polycarbonate-grafted poly(ethylene glycol) methacrylate-based gels,[28,29] cationic betaine ester-based gels,[30] ε-poly-L-lysine-based gels,[31] and self-assembled gels from amino acids or peptides[26] or through supramolecular interaction[32] were developed with potential biomedical applications specially antibacterial activity.[33,34] They can kill microorganisms and inhibit biofilm formation through a trap-and-kill-,[35] contact-active-,[36,37] or release-based pathway.[38] The contact-active mechanism is applicable to amino acid, peptide, or antimicrobial peptides (AMPs) based gels where the drug is not incorporated through physical or reversible chemical bond. In hydrogels that destroy microorganisms by the releasing mechanism, their active released components have also been urbanized by fragmented antibiotics, metal nanoparticles, or AMPs.[39,40]

In spite of having several reports of antibacterial gels, their cellular-matrix-dependent activity is yet to be explored. As the human body consists of all-solid, semisolid, and liquid matrices,[41] there is an imperative requirement to develop a potent PAC-based 3D network to fight with pathogenic microorganisms such as bacteria in several matrices having all the superiority of the gel framework and PACs. Hence, herein we have designed and synthesized a potential antibiotic, ciprofloxacin-based hyperbranched polymeric hydrogel composed of polyethylene glycol methyl ether methacrylate (PEGMA) and sulphabetaine methacrylate (SBMA) units, and we explored in detail matrix-dependent antibacterial activity against novel Gram negative *Vibrio chemaguriensis* Iso1 (*V. chemaguriensis*) strain with the proposed mechanistic elucidation. This novel strain is resistant to most of the common antibiotics and may be potentially pathogenic as the closest phylogenetic relatives such as *V. alginolyticus*, *V. parahemolyticus*, *V. harveyi*, and other members of the *Vibrio harveyi* clade harbor many pathogenic gene islands and thus can pose a serious threat in future to humans under opportunistic conditions.[42] Moreover, many of the genes linked to pathogenecity have been also found in *V. chemaguriensis*. Greater antibacterial efficacy in solid matrix was resulted from potential release of thiol-terminated active antibiotic fragment and direct contact with the cell wall.[43] The bacterial cell morphology transformed from rod to sphere leading to chain formation. On the contrary, matrix-assisted inhibition of antibacterial activity was observed in liquid medium. The bacterial surface area was enhanced and thick exopolysaccharide (EPS) was generated,[44] induced by released component from gel with corresponding entrapment in EPS. Preliminary study was also extended with linear random copolymer composed of same components analogous to gel and against another series of pathogenic strains; Gram-negative *Vibrio alginolyticus* (*V. alginolyticus*), *Escherichia coli* (*E. coli*) XL10 and Gram-positive *Staphylococcus aureus* (*S. aureus*). PEGMA was employed to incorporate considerable extent of hydrophilicity enhancing the antibacterial properties,[45] and zwitterionic SBMA introduced antibiofilm characteristics of the gel leading to biopassive killing efficacy of bacteria.[46]

RESULTS AND DISCUSSION

Polymer Design and Synthesis. We have used reversible addition−fragmentation chain transfer (RAFT) polymerization to prepare linear random copolymers and gels using SBMA and PEGMA monomers in methanol (MeOH) at 65 °C using 2,2′-azobis(isobutyronitrile) (AIBN) as radical initiator. For RAFT polymerizations, four different chain transfer agents (CTAs) were used leading to generation of two linear and two hyperbranched polymers, and the results are summarized in Table 1. Two CTAs such as *tert*-butyl carbamate (Boc)-

Table 1. Results from the Synthesis SBMA- and PEGMA-Based Linear and Hyperbranched Copolymers via RAFT Polymerization at 65 °C in MeOH[a]

polymer	[M]/[CTA]/[AIBN]	SBMA content in feed	conv.[f] (%)	$M_{n,theo}$[g] (g/mol)	$M_{n,UV}$[h] (g/mol)
LSP[b]	80/1/0.2	60	92	21300	22500
HBSP[c]	80/1/0.2	60	87	20000	22200
CLSP[d]	80/1/0.2	60	88	21000	22300
CHBSP[e]	80/1/0.2	60	95	22500	-

[a]Polymerization time = 24 h. [b][Monomer (M)]/[CTA]/[AIBN] = [SBMA+PEGMA]/[BBHT]/[AIBN]. [c][M]/[CTA]/[AIBN] = [SBMA+PEGMA]/[VBHT]/[AIBN]. [d][M]/[CTA]/[AIBN] = [SBMA+PEGMA]/[Boc-cipro BBHT]/[AIBN]. [e][M]/[CTA]/[AIBN] = [SBMA+PEGMA]/[Boc-cipro VBHT]/[AIBN]. [f]Calculated gravimetrically. [g]$M_{n,theo}$ = (([monomer]/[CTA] × average molecular weight (MW) of monomer × conversion) + MW of CTA). [h]$M_{n,UV}$ = Determined by UV−vis study.

ciprofloxacin *S*-benzyl *S*′-hydroxyethylthiocarbonate (Boc-cipro BBHT) and Boc-ciprofloxacin *S*-(4-vinyl)benzyl *S*′′-hydroxyethylthiocarbonate (Boc-cipro VBHT) were prepared by condensation reaction of Boc-ciprofloxacin (see ^{1}H NMR in Figure S1) with *S*-benzyl *S*′′-hydroxyethylthiocarbonate (BBHT) and *S*-(4-vinyl)benzyl *S*′′-hydroxyethylthiocarbonate (VBHT) respectively by using dicyclohexylcarbodiimide (DCC) as water scavenger and catalytic amount of 4-(dimethylamino)pyridine (DMAP) (Scheme S1). The Boc-cipro BBHT and Boc-cipro VBHT were characterized by ^{1}H NMR spectroscopy (Figure S2) and electrospray ionization mass spectrometry (ESI-MS) (Figure S3 and S4). The major fragment observed for both the CTAs are same with $[M + Na]^+$ = 413.45 for Boc-cipro BBHT and 413.64 for Boc-cipro VBHT. They correspond to the terminal thiolated fragment of those CTAs.

SBMA and PEGMA were copolymerized via RAFT technique in MeOH at 65 °C using AIBN, Boc-cipro BBHT and BBHT as CTAs (Scheme 1) at [SBMA+PEGMA]/[CTA]/[AIBN] = 80:1:0.2 with a particular monomer feed composition. The characterization results for these polymerization reactions are shown in Table 1. The two copolymers were represented as LSP and CLSP where L, S, P and C represent linear, SBMA, PEGMA units and Boc-cipro BBHT CTA, respectively. The structure of LSP and CLSP were characterized by ^{1}H NMR spectroscopy (Figure S5). For these polymers, theoretical molecular weight ($M_{n,theo}$) was determined by using the formula; $M_{n,theo}$ = (([monomer]/[CTA] × average molecular weight (MW) of monomer × conversion) + MW of CTA). The copolymers demonstrated the expected

DOI: 10.1021/acs.bioconjchem.8b00846
Bioconjugate Chem. 2019, 30, 218−230

Scheme 1. Synthesis of SBMA- and PEGMA-Based Linear Random Copolymers: LSP, CLSP and Deprotected DCLSP; Hyperbranched Copolymers: HBSP, CHBSP, and Deprotected DCHBSP in Absence and Presence of Ciprofloxacin, Respectively, by RAFT Polymerization

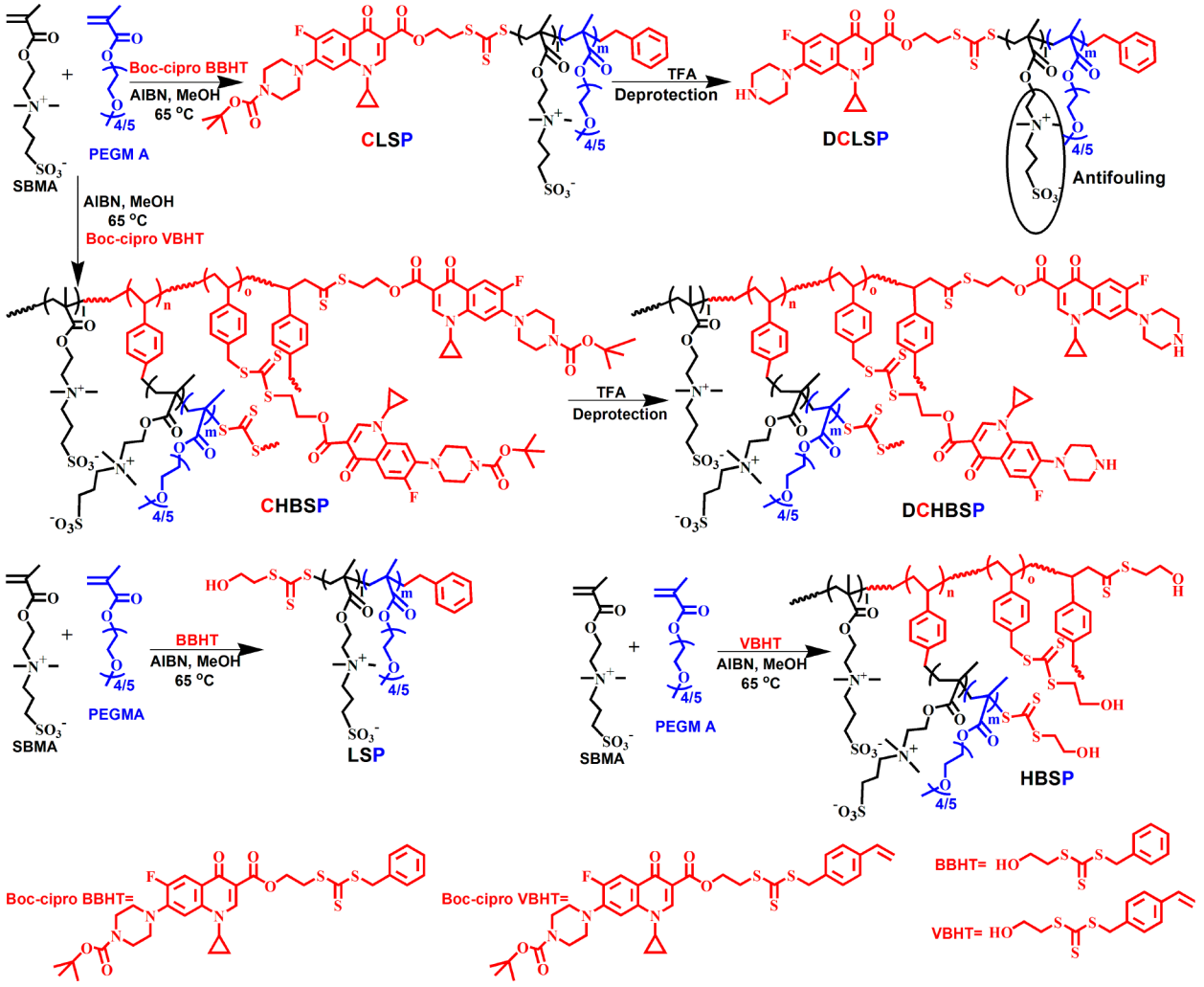

absorption for the trithiocarbonate moiety at λ_{max} = 307 nm, indicating the retention of ω-trithiocarbonate group of CTAs in the polymer chain end during the RAFT polymerization (Figure S6).[47] From UV−vis spectroscopy, molecular weight ($M_{n,UV}$) values were determined (see Supporting Information), which are in good agreement with the $M_{n,theo}$ values. Boc group deprotection from the ciprofloxacin moiety of CLST generated the original antibiotics form attached to the polymeric main chain with enhanced water solubility and represented as DCLST where D stands for deprotection. The other linear polymer LSP also exhibited nice water solubility due to the presence of considerable extent of zwitterionic SBMA in the polymer.

Copolymerization via RAFT technique of SBMA and PEGMA resulted in a hyperbranched architecture, where polymerization reactions were performed in MeOH at 65 °C using Boc-cipro VBHT and VBHT as CTAs (Scheme 1) at [SBMA+PEGMA]/[CTA]/[AIBN] = 80:1:0.2. Selective usage of Boc-cipro VBHT transformed the polymeric solution into a fragile chemical irreversible gel within 2 h without addition of cross-linker. The major driving force may be an extensive $\pi-\pi$ stacking and hydrogen bonding interaction which can fold the polymeric chain into a 3D gel matrix.[48] Though the gelation time for the gel was 2 h, it was synthesized for 24 h to attain maximum monomer conversion (Table 1). The gel exhibits good swelling capacity in dichloromethane (DCM) or chloroform ($CHCl_3$) but weak efficiency in hexane. The deprotection of Boc functionality caused transformation of an organogel to a hydrogel with a considerable swelling efficacy in water.[49] Substantial dye adsorption capacity was confirmed by the rhodamine B adsorption experiment leading to further visual clarification supporting gel formation through inversion experiment (Figure S7). The hyperbranched copolymer was represented as HBSP, and the polymeric gel was designated as CHBSP, where C, HB, S and P correspond to Boc-cipro VBHT, hyperbranched, SBMA and PEGMA units, respectively. The Boc deprotected form of CHBSP was named as DCHBSP containing the original ciprofloxacin form, where D stands for deprotection. The structure of HBSP was characterized by ^{1}H NMR spectroscopy (Figure S5). The copolymer demonstrated the expected absorption for the trithiocarbonate moiety at λ_{max} = 307 nm, indicating the retention of ω-trithiocarbonate group in the polymer. The $M_{n,UV}$ value determined from UV−vis spectroscopy matches nicely with the $M_{n,theo}$ value (Table 1).

Swelling Properties of DCHBSP Hydrogel. Water was chosen to investigate the solvent uptake behavior of the

DOI: 10.1021/acs.bioconjchem.8b00846
Bioconjugate Chem. 2019, 30, 218−230

synthesized polymeric hydrogel, DCHBSP, and swelling ratio (SR) was calculated with a measured amount of hydrogel taken in a beaker (see Supporting Information). Maximum swelling was achieved at 15 h with a SR value of 9.7 (Figure S8A). However, after achieving an equilibrium SR value, a gradual decrease of swelling degree was observed up to 22 h (Figure S8A). Initially, the osmotic imbalance in water was enhanced between the interior and exterior of the gel matrix, which accelerates the high degree of swelling by ionic dissociation.[50] Then, repulsion of hydrophobic phenyl groups became prominent leading to a diminished osmotic effect that caused the continuous deswelling of gel. Also, because of the fragile nature of the gel, the network was not so firm to retain highest equilibrium swelling degree over long period of time, and as a result, deswelling starts to some extent after reaching the equilibrium value.

The water retention kinetics of DCHBSP polymeric hydrogel was also studied by investigating the evaporation of solvent (H_2O) from the equilibrium swollen gel in air at room temperature as a function of time (Figure S8B). The rate of solvent evaporation was sufficiently slow and almost 12 h was taken to achieve the constant equilibrium value (0.13). However, the weight of the dry gel dropped nearly 50% (33.4 mg) of its initial dry weight (60.0 mg) after 24 h, proceeding through complete deswelling. This phenomenon actually evidenced the active and sustained release of some covalently bonded fragments during deswelling process, hence causing subsequent mass loss.

Rheological Property of Deprotected Hydrogel. The mechanical properties of DCHBLP gel can be well understood by studying rheology. Measurement of storage modulus (G') and loss modulus (G'') versus angular frequency (ω) was performed under a constant applying strain of 0.1%. The expected mechanical behavior of 3D network was established by the higher value of G' than G'' over the measured frequency range for the hydrogel represented by Figure 1.

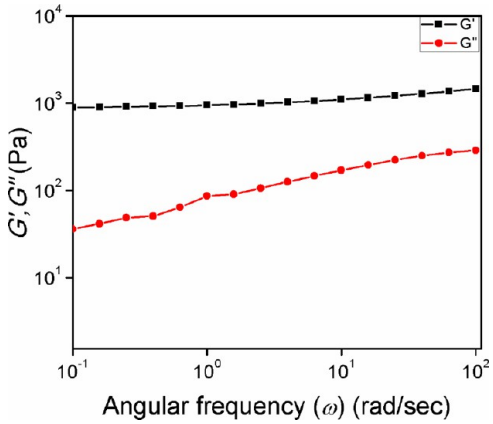

Figure 1. Storage modulus G' and loss modulus G'' versus frequency (ω) (strain 0.1%) of the DCHBSP gel.

Time-Dependent Long-Lasting Release of Ciprofloxacin Derivative from DCHBLP Gel. Incorporation of several antibiotics into 3D cross-linked network through noncovalent or reversible covalent interactions is well studied in the literature.[51] In those cases, expected sustainable release of antibiotics from the hydrogel matrix can lead to a long-lasting antibacterial activity.[52] Hence, we have studied the ciprofloxacin release kinetics at pH 8.0 from the DCHBLP gel, where the antibiotic part was incorporated into the gel through ester linkage and played a major role in gel formation. The particular pH was chosen as our major point of interest, *V. chemaguriensis*, the novel strain that have genes linked to pathogenicity, can grow rapidly at pH 8.0. Bare ciprofloxacin provided three UV absorbance peak at 236, 275, and 318 nm (Figure 2A).[53] However, coupling with trithiocarbonate-based CTA portrays a considerable blue shifting in the peak positions at 206, 260, and 312 nm, as shown in Figure 2A.

Initial release study provided an increasing absorbance with time where the peak intensities at 206 and 312 nm are dominant, and the 260 nm peak became suppressed as shown in Figure 2B (also see the inset). The primary release was actually regulated by the swelling of the gel with a slightly higher proportion of ciprofloxacin-based component discharge in first 2 h. This is similar to the swelling kinetics of DCHBSP gel, where we observed sharp change in SR value in the first 2 h. Maximum peak intensity at 312 nm was observed at 20 h (Figure 2B), when the swelling almost completed and reached to equilibrium (Figure S8A).

The day-wise release kinetics was performed upon achieving equilibrium swelling of the gel (i.e., after keeping the gel in water for 24 h). The gel showed sustainable release of antibiotics fragment over 7 days, mostly regulated by the equilibrium swelling deswelling process through breakage of covalent bond. This study indicated a decrease of peak intensity at 312 nm and another major characteristic band of ciprofloxacin derivative at 260 nm appeared dominantly with enhanced intensity (Figure 2C). For better understanding about the chemical structure of ciprofloxacin based active fragment, 2-ethanolamine induced degradation of Boc-cipro VBHT was performed to convert trithiocarbonate end group to thiol via aminolysis[54] (Scheme S2). The yellow color of the solution disappeared after complete disintegration, and UV–vis spectroscopy verified the consumption of CTA group through disappearance of the absorption peak at 311 nm (Figure 2D). This reaction actually generated a terminal thiol-containing ciprofloxacin fragment (Scheme S2), which shows same characteristics absorbance peak as the day-wise-released component. This experiment confirmed the chemical structure of released active fragment, which is thiol-terminated ciprofloxacin component. The structure as a result of the most feasible disintegration was further evidenced by ESI-MS spectra of both ciprofloxacin-based CTAs (Figures S3 and S4).

When the buffer solution on the gel was replaced with fresh buffer after complete swelling, the gel became collapsed with a total removal of active ciprofloxacin fragment instead of sustainable release due to its fragile nature. The superiority of our antibiotic-based hydrogel originates from the release of active fragment both during swelling and deswelling via the discharge of thiol-terminated ciprofloxacin fragment through breakage of covalent linkage. Generally drug carrier gels with physically and chemically entrapped antibiotics exhibited their release capacity during deswelling kinetics.[55,56] The bioactivity of released antibiotics fragment should be retained to exhibit an antibacterial effect, which was further tested against *V. chemaguriensis*.

Diffusion- and Contact-Based *In Vitro* Antibacterial Activity. Zone of inhibition (ZOI) experiments were conducted to establish the diffusion of active antibiotic fragments during the swelling and deswelling process from the DCHBSP hydrogel, along with other three polymers; LSP, HBSP, and DCLSP up to 600 μg/mL against several bacterial

DOI: 10.1021/acs.bioconjchem.8b00846
Bioconjugate Chem. 2019, 30, 218–230

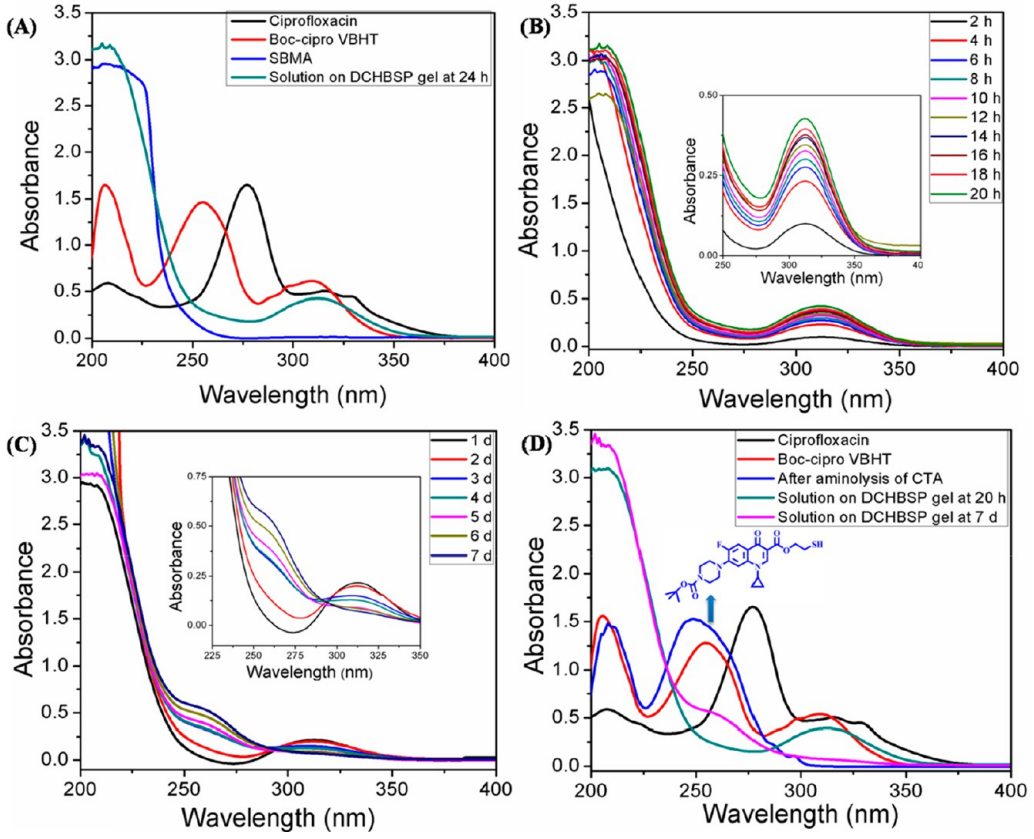

Figure 2. (A) UV−vis absorbance spectra of ciprofloxacin, Boc-cipro VBHT, SBMA, and water solution of DCHBSP gel after 24 h; (B,C) time-dependent release study of ciprofloxacin fragments from the DCHBSP gel; (D) UV−vis absorbance spectra of Boc-cipro VBHT before and after aminolysis along with free ciprofloxacin, gel-containing solution at 20 h and 7 d for comparison.

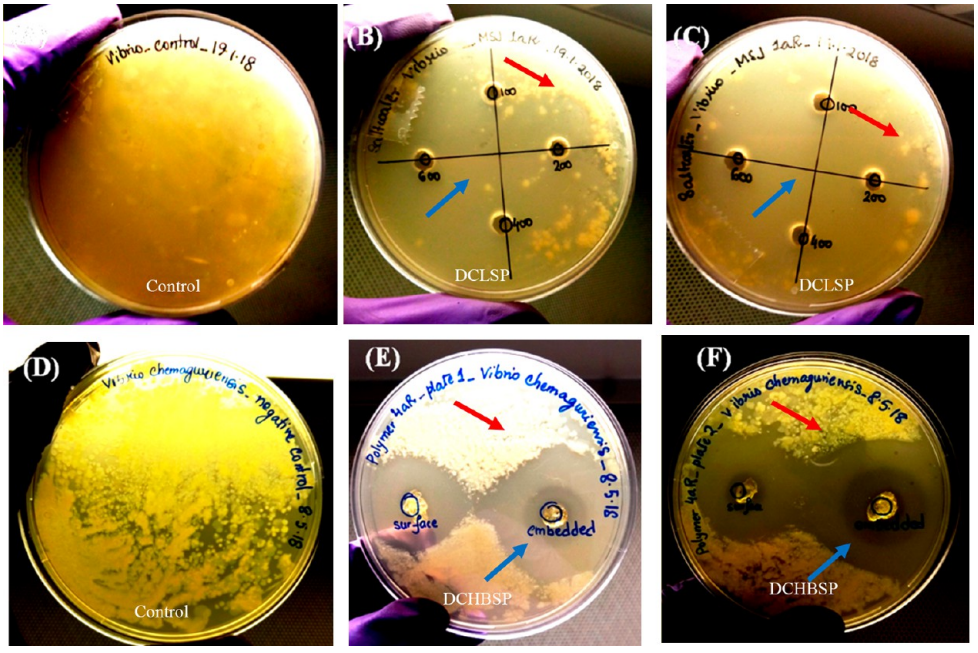

Figure 3. Antibacterial activity of the synthesized polymers against *V. chemaguriensis* by zone of inhibition experiment: (A) and (D) control show (without polymer) where bacterium was grown in the complete absence of the polymers. (B) and (C) show action of DCLSP polymer. Clear areas seen on the plate indicate regions where bacterium could not grow. The red arrow shows growth of bacterium along the periphery of the plate in regions where the polymer effect is minimal. The numbers 100, 200, 400, and 600 show concentration (μg/mL) of DCLSP polymer. (E) and (F) show action of DCHBSP of 30 mg dry weight of gel. The blue arrow shows the zone of clearing resulting from inhibitory action of the polymer against cell growth. The gel was kept in contact with the surface of the agar and embedded in the agar plate.

DOI: 10.1021/acs.bioconjchem.8b00846
Bioconjugate Chem. 2019, 30, 218−230

Table 2. Quantitative values of zone of inhibition against *E. coli*, *S. aureus* and pathogenic *V. chemaguriensis*.

polymer	concentration (μg/mL)	radius of zone of inhibition (cm) (R_1)[a]			zone of inhibition (cm^2)		
		E. coli	*S. aureus*	*V. chemaguriensis*	*E. coli*	*S. aureus*	*V. chemaguriensis*
DCLSP	100	0.00	0.00	0.70	0.00	0.00	1.54
	200	0.00	0.00	1.50	0.00	0.00	7.06
	400	0.00	0.00	2.20	0.00	0.00	15.19
	600	0.00	0.00	2.40	0.00	0.00	18.08
DCHBSP (embedded in the surface)	solid (30 mg)	ND[b]	ND	2.40	ND	ND	18.08
DCHBSP (gel on the surface of the plate)	solid (30 mg)	ND	ND	2.10	ND	ND	13.84

[a]zone of inhibition = πR_1^2. [b]ND = not determined.

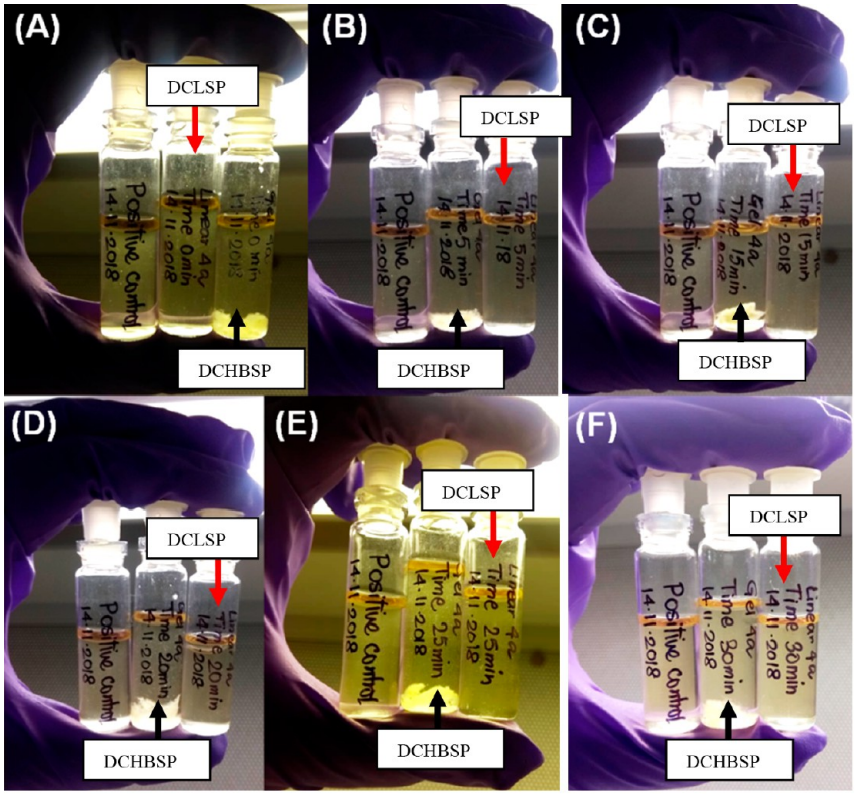

Figure 4. Comparative activity of DCHBSP (gel 4a) and DCLSP (linear 4a) against *V. chemaguriensis* in liquid matrix at (A) 0, (B) 5, (C) 15, (D) 20, (E) 25, and (F) 30 min time intervals. The turbidity corresponding to cell growth was qualitatively similar between the positive control vials and the ones treated with polymer DCLSP. The vials containing cells treated with DCHBSP polymer showed less turbidity indicating possible inhibition to cell growth due to presence of the polymer.

strains; *E. coli*, *S. aureus*, and novel pathogenic *V. chemaguriensis* (Figures S9–S11 and 3). Antimicrobial effect of DCHBSP gel was tested by adhering 30 mg of gel to the surface along with embedding 30 mg gel in Luria broth (LB) agar plate (Figure 3). The bacterial isolates were then incubated at 37 °C for 12–16 h. LSP and HBSP did not show any ZOI (Figures S9 and S10; show no inhibitory action of LSP and HBSP polymers against *E. coli*, *S. aureus* and *V. chemaguriensis*), whereas ciprofloxacin bearing linear random copolymer (DCLSP) and hyperbranched hydrogel (DCHBSP) displayed significant clearance zone against *V. chemaguriensis* (Figure 3). Interestingly, DCLSP also did not show any inhibition on the growth of *E. coli* and *S. aureus* (Figure S11 shows no zone of clearing following treatment with DCLSP at 100, 200, 400, and 600 μg/mL concentrations). This result confirmed the potential of bioactive terminal thiol-containing antibiotic fragment to display promising antibacterial effect against pathogenic strain both for ciprofloxacin based linear polymer or hyperbranched gel. Interestingly, the linear DCLSP showed antimicrobial effects at concentration as low as 100 μg/mL (4.5 μmolar). In our previous work, we have already explored the efficacy of hyperbranched architecture on antibacterial activity over the linear one.[57] Hence, major attention was paid to the ciprofloxacin based hyperbranched gel and its bactericidal activity. The significant zone of inhibition might have originated by the diffusion of bioactive antibiotic fragment into the surroundings, thereby inhibiting cell growth in solid matrix. Possible "forced bacterial cell wall to gel surface contact" in the solid matrix could be an additional factor contributing toward antimicrobial properties of this polymer.[58] These combined mechanistic effects could have resulted in the displayed antibacterial activity of this polymer. Table 2 provides quantitative data of the area of ZOI.

Release-Based *In Vitro* Antibacterial Activity. To study the efficacy of the hyperbranched gel in the liquid medium versus the solid matrix, matrix-dependent antimicrobial activity

DOI: 10.1021/acs.bioconjchem.8b00846
Bioconjugate Chem. 2019, 30, 218–230

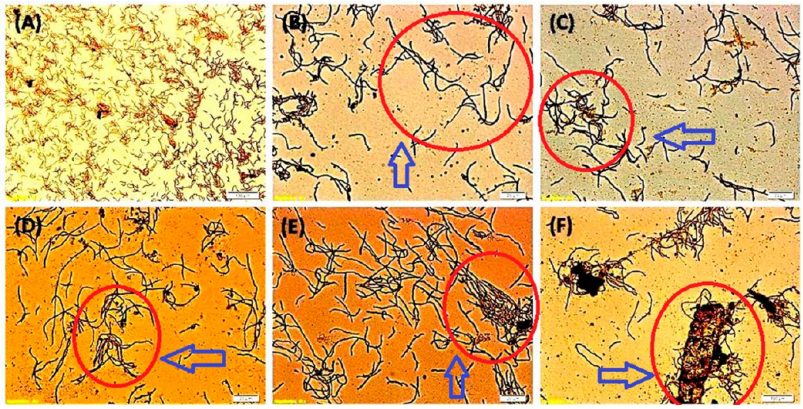

Figure 5. Optical microscopy images of pathogenic *V. chemaguriensis* upon treatment with DCHBSP gel: (A) control (without polymer treatment) at 25 min, (B) 0, (C) 5, (D) 10, (E) 15, and (F) 25 min at 40× resolution. Blue arrows and red circles are marked to indicate crumpling and lengthening of cells under treatment.

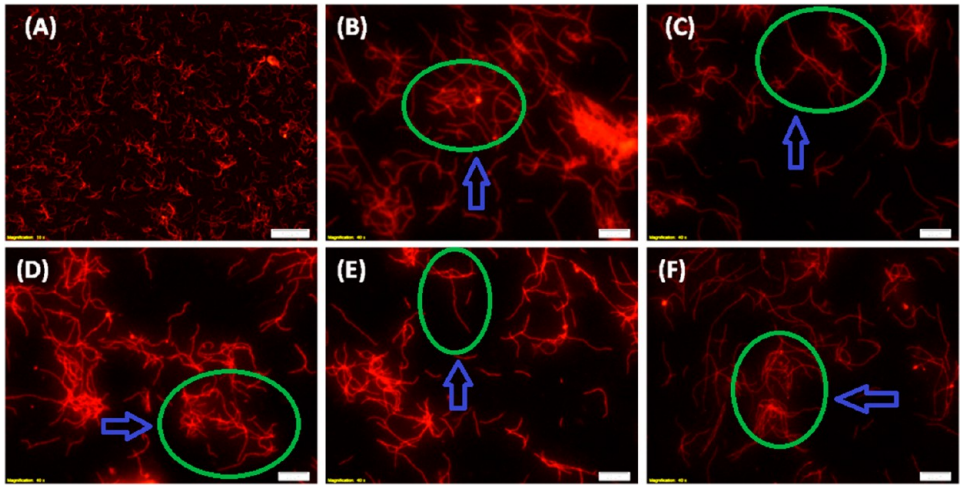

Figure 6. Epifluorescence microscopy images of pathogenic *V. chemaguriensis* upon treatment with DCHBSP gel: (A) control (without polymer treatment) at 25 min, (B) 0, (C) 5, (D) 10, (E) 15 and (F) 25 min at 40× resolution on staining with acridine orange. Blue arrows and green circles are marked to indicate crumpling and lengthening of cells under treatment.

against *V. chemaguriensis* was further explored in liquid medium. Use of liquid medium or broth provides a matrix that allows shift mixing and dispersion of antimicrobial agents. The overnight-growing *V. chemaguriensis* culture (200 μL, OD_{600} = 0.5) was diluted with fresh LB broth (3 mL) containing 30 mg of DCHBSP gel (10 mg/mL). The culture did not show any growth in the presence of gel. The *V. chemaguriensis* culture in LB medium at pH 8.0 and salinity 11.5 was taken as positive control (Figure S12). At comparative concentrations of the polymers, greater antibacterial activity was demonstrated by the DCHBSP in the gel form in the liquid matrix. This could be clearly seen from the growth inhibition observed in Figure S12, where no growth of *V. chemaguriensis* could be observed by treatment of DCHBSP, but complete cell growth inhibition is not observed by treatment of DCLSP. Though complete inhibition was not observed under the gel treated environment, greater bactericidal efficacy than that of the linear analogous DCLSP could be clearly determined using a liquid matrix qualitatively as shown in Figure S12. Lower turbidity of the gel-treated culture in comparison to DCLSP-treated culture qualitatively indicated great antimicrobial efficiency of the gel.[59] The activity of DCHBSP and DCLSP in liquid matrix was compared qualitatively by performing time-dependent growth experiment at different time point up to two generations of *Vibrio* (up to 30 min) (Figure 4 and S13). Little difference in turbidity was observed here also at different time points, exhibiting slightly greater activity of gel in liquid matrix. We speculate that the 3D gel architecture could be a possible factor determining the increased efficiency of the gel.[57] Greater inhibition by DCHBSP gel as observed in the solid matrix could result from both the forced contact active mechanism and the release-based mechanism that caused a bacterial killing effect. In the liquid matrix, the active ciprofloxacin fragment released from gel swelling and deswelling could be the only determining factor that resulted in the observed inhibition of bacterial growth.

Since the release of the "active factor" contributing to antimicrobial activity of DCHBSP gel could be a time-bound process, it was monitored over 30 min in liquid medium (Figures S14 and S15) to determine the antibacterial activity from released medium component and cell morphology was visualized using optical microscopy of the studied bacterial strains collected at different time intervals. The experiment was performed against two *Vibrio* strains, *V. alginolyticus*, and *V. chemaguriensis* until 30 min to trap any change during the

DOI: 10.1021/acs.bioconjchem.8b00846
Bioconjugate Chem. 2019, 30, 218−230

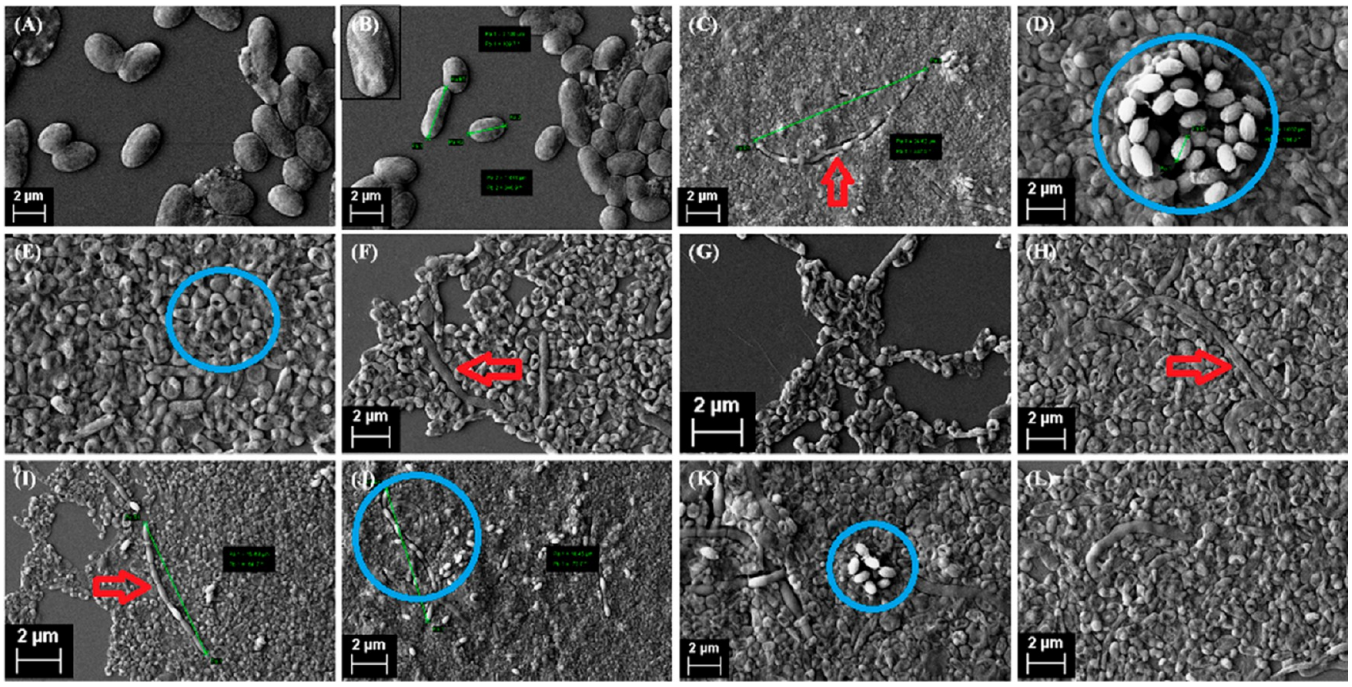

Figure 7. FESEM images of *V. chemaguriensis* cells: (A), (B) control, (C)−(G) treated with DCHBSP gel within the ZOI, (H)−(L) treated with DCHBSP away from the ZOI. Red arrows indicate the longer cells; rod to sphere morphology changing and chain formation of cells are shown by blue circles.

doubling log phase up to two generation since cell doubling time in log phase for *Vibrio* is nearly 15 min. In Figures S14A,B, the displayed complete bactericidal effect against *V. alginolyticus* might be a consequence of released active ciprofloxacin fragment transportation into the bacteria cell and thus lead to genetic components entrapment causing cellular death, which is a common mechanism of known antibiotics.[60] The similar transport of the released bioactive part from DCHBLP gel was mostly restricted in the case of *V. chemaguriensis* (Figure S14C) because of their potential production of thick EPS layer over the cell which inhibited bactericidal efficacy by entrapment of active released component, which was further explored and confirmed by transmission electron microscopy (TEM) analysis (*vide infra*).

Collected cells of *V. chemaguriensis* at time points 0, 5, 10, 15, and 25 min from DCHBSP-gel-treated liquid matrix were observed by optical and epifluorescence microscopy approaches after selective staining with nucleic acid.[61] The cells appeared to form chains and clumps upon treatment with DCHBSP gel. Such features were not observed in the control where cells were not exposed to the polymer (Figure 5). Formation of chains and clumps indicates uncontrolled cell division, thus reflecting the possibility of uncontrolled regulation of shape, elongation, division, and sporulation (SEDS) family of proteins within bacterial cells. The appearance of chain formation could also indicate that the cells were trying to increase surface area to cope up with stress generated from the polymer. This could also enhance additional uptake of nutrients for survival during stress phase.

Epifluorescence microscopic images using acridine orange stain also provided similar observations (Figure 6). Staining by specific stains that bind to cellular components such as the cell membrane and nucleic acid within the studied bacteria is shown in Figures S16−S18. Figure S16 highlighted *V. chemaguriensis* cells after staining with fluorescein-5-isothiocyanate (F143), 4′,6-diamidino-2-phenylindole (DAPI) and superimposed dual staining after treatment with DCHBSP gel at 15 and 25 min intervals. The green color observed under the epifluorescence microscope indicates binding of F143 to cell membrane whereas the blue color indicates binding of DAPI to the nucleic acids. Upon prolonged exposure to DCHBSP gel, the amount of nucleic acid appeared to become compact as observed from decrease in intensity of the DAPI stain over time. However, no change in intensity of F143 was observed over time with the polymer exposure. This indicates that the cell membrane may not be a potential target site of the polymer. The polymer may be inhibiting steps of DNA replication which could result in the decrease in cell size and subsequent increase in generation time of the studied bacterium. Increase in doubling time could explain the decrease in growth observed over time. However, as the polymer did not completely kill the bacterium, there is a possibility that it could be mediating its antimicrobial properties by inhibiting key enzymes involved in DNA replication. Such mode of actions by hyperbranched polymers could be further explored to understand their antimicrobial properties.

Morphological Clarification. When bacterial cells are exposed to antibiotics or antibacterial agents, cell surface area generally increases because of deformation of the cell wall, cell membrane, or nucleic acid related to cell lengthening, stacking, and crumpling.[62] Cell morphology could be distinctly observed by field emission-scanning electron microscopy (FESEM) and transmission electron microscopy (TEM) imaging. As DCHBLP gel displayed greater antibacterial effect in solid matrix compared to liquid one, FESEM and TEM imaging were undertaken with the cell pellets collected from treated LB agar plate near ZOI and periphery of the plate to compare with control cell morphology. Rod to sphere transformation of the cells followed by chain formation was clearly observed under

DOI: 10.1021/acs.bioconjchem.8b00846
Bioconjugate Chem. 2019, 30, 218−230

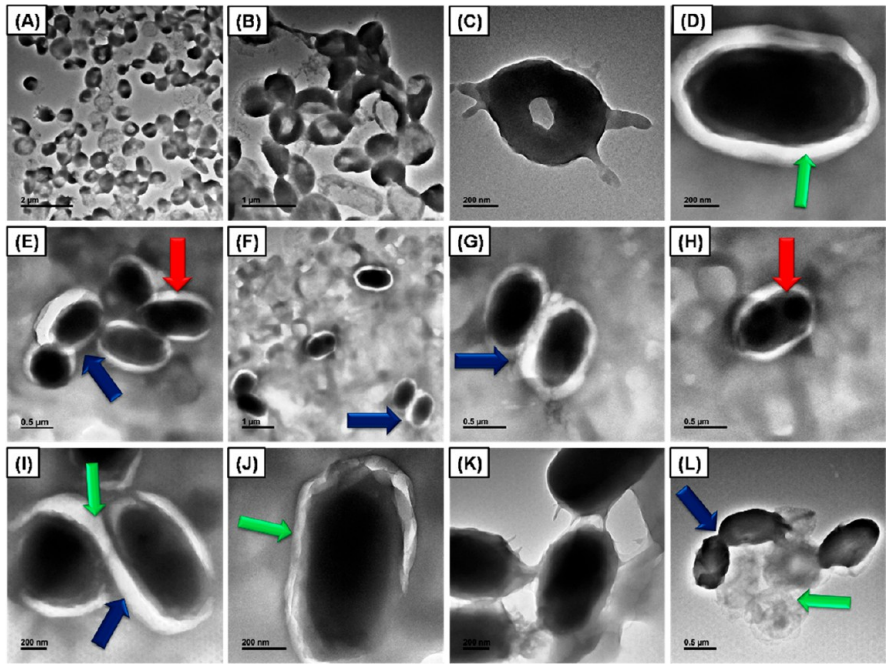

Figure 8. TEM images of *V. chemaguriensis* cells: (A), (B) and (C) control, (D)−(H) treated with DCHBSP gel within the ZOI, (I)−(L) treated with DCHBSP away from the ZOI. Green arrows indicate thick EPS. Red arrows indicate chromosomal cleavage of cell and blue ones indicate cell emerging to increase the surface area under treated condition.

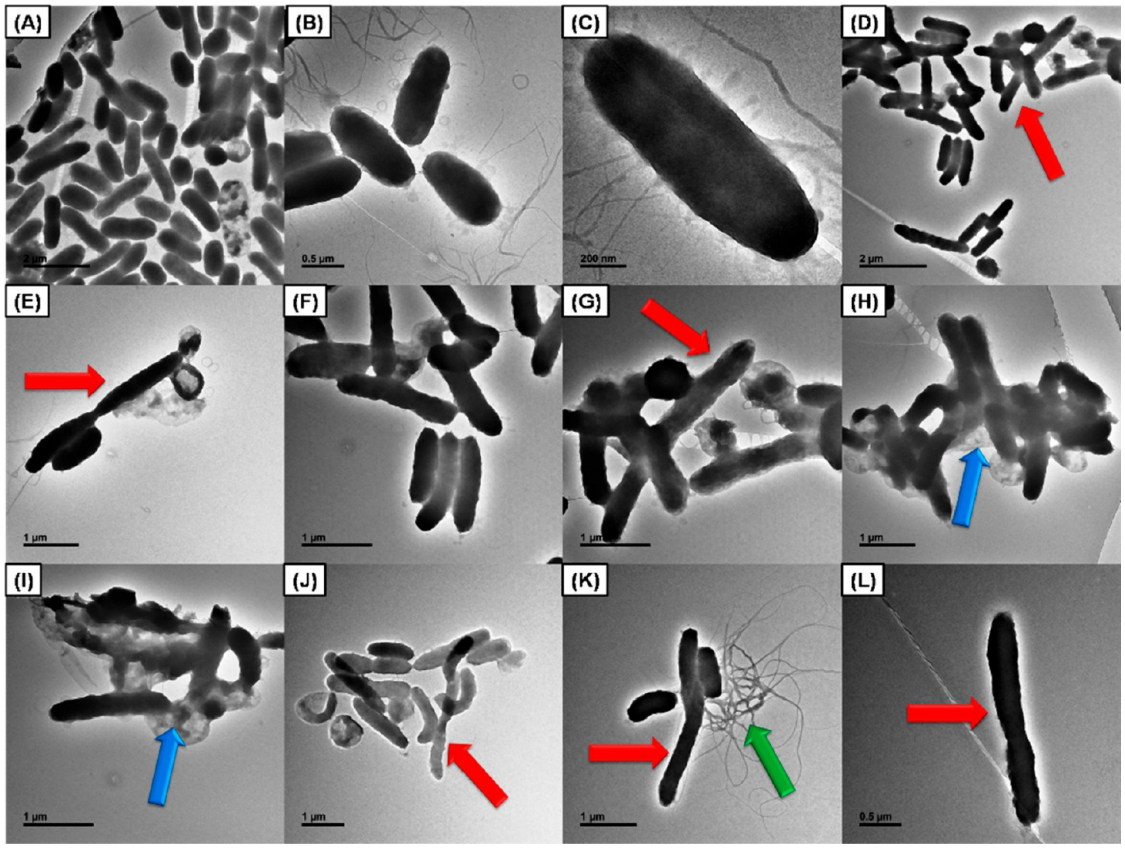

Figure 9. TEM images of *V. chemaguriensis* cells collected from overnight culture: (A), (B) and (C) control, (D)−(L) treated with DCHBSP gel. Red arrows indicate cell emerging to increase the surface area through lengthening and stacking, and blue arrows indicate thick EPS under treated condition. Entrapment of active ciprofloxacin fragment by EPS layer is indicated by green arrows.

treatment for both near and far from the clearance zone by FESEM analysis indicating widespread effect of the released component (Figure 7). As observed in Gram staining and acridine orange staining, FESEM also indicated chain

DOI: 10.1021/acs.bioconjchem.8b00846
Bioconjugate Chem. 2019, 30, 218−230

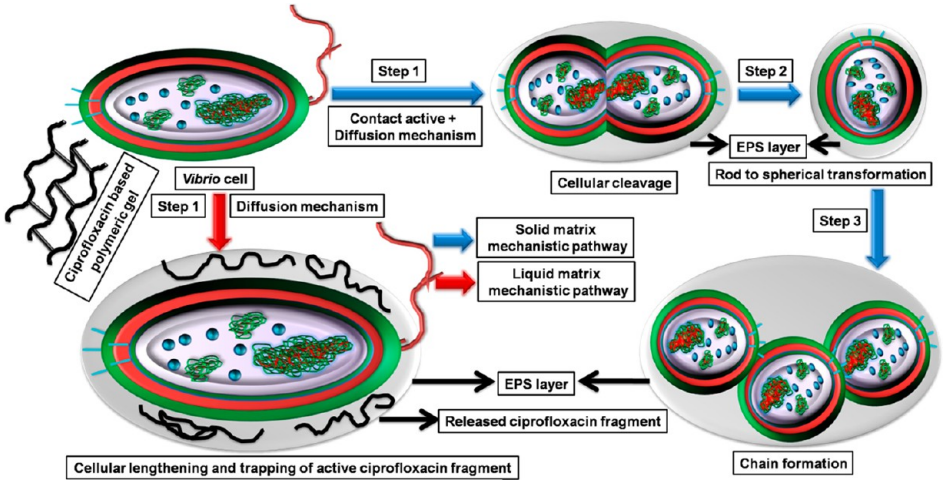

Figure 10. Schematic representation of bactericidal mechanism of DCHBSP gel (ciprofloxacin-based polymeric gel) against *V. chemaguriensis* strains in solid and liquid matrices.

formation and clumping under the influence of the polymeric gel. This indicated that the polymer was bacteriostatic in nature. As known for ciprofloxacin and related drugs, the "active fragment" of this hyperbranched polymer appears to inhibit septum formation thereby inhibiting the mother cell from completely dividing into two daughter cells.[63] These observations were further reinstated by TEM imaging. Additionally, a thick layer of "exopolysaccharide-like" material appears to form a sheath on the cells (Figure 8). Further analysis would be required to qualitatively prove that this "exopolysaccharide-like" material is an important component of the biofilm. The formation of a biofilm could act as a possible defense mechanism employed by bacterial cells to inhibit entry of polymer inside the cells. Interestingly, chain formation and cellular clumping was not observed in cells grown in broth with the addition of polymer. TEM images did not show any observable difference between cells from control and cells under polymer influence, although the presence of thick "exopolysaccharide-like" material was also observed here.

TEM analysis was also performed with treated bacterial cells representing *V. chemaguriensis* collected from liquid matrix which displayed matrix-assisted inhibition of antibacterial activity. On the other hand, cellular morphological switching was not observed (Figure 9). Lengthening of the cells to enhance surface area and thick EPS generation were observed using TEM approach. The entrapment of released component by thick EPS matrix was observered (Figure 9K), and this impeded the polymer contact with cell membrane, having no effect on observable morphology.

Proposed Mechanistic Elucidation. *V. chemaguriensis* is a novel Gram-negative bacterial strain with the ability to express pathogenicity and contains an inner membrane, peptidoglycan, and outer membrane as well as resistant to most of the common antibiotics. Presently known antimicrobial agents are often rendered ineffective against pathogenic bacteria. Drug-resistant bacteria are known to employ several methods to "save" themselves against known antibiotics. These mechanisms include the production of enzymes such as β-lactamase, which can cleave the β-lactam rings of antibiotics. Some bacteria are also known to have robust efflux mechanisms that "throw" antibiotics out of the bacterial cells. Such defense mechanisms rendered by pathogenic bacteria often hamper treatment through antibacterial therapeutics such as in case of nosocomial infection.

Antibacterial activity of a gel material can originate by diffusion-based release, contact-active, or trap-and-kill mechanisms. The "trap-and-kill" mechanism appears to be an effective way of increasing the efficacy of antimicrobial agents. Gel materials, such as the hyperbranched polymer designed in this study, could potentially be used as a "trap-and-kill" antimicrobial agent. Generally, a cationic gel not bound with antibiotics, could kill upon contact with bacterial cells. Attaching antibiotics to cationic gels either through physical or chemical bonds readily form 3D frame works. Time-bound release of the "active fragment" through diffusion appears to provide a more efficient antimicrobial mechanism. In our framework, ciprofloxacin is covalently bonded through ester linkage. On the other hand, production of a clear ZOI around the gel embedded to the plate clearly pointed toward the contact-active mechanism. This forceful contact between bacterial cell wall and the gel surface containing the active component can only happen in the solid plate matrix, not in liquid broth where *Vibrio* cells are in rapidly growing condition. This "dual" mechanism is actually responsible for the complete bactericidal effect in solid matrix and rod to spherical transformation with intact cell wall leading to chain formation is totally induced by forced contact mechanism as schematically represented in Figure 10. In broth, lowering of bacterial growth only happened via diffusion of active antibiotic fragment. After a certain time, the production of an additional EPS layer appears to bind with the released active antibiotic fragment thereby keeping intact cell morphology. Formation of procular bodies as seen in TEM could also be a cellular mechanism that could confer resistance from contact active antimicrobial mechanism (Figure 9). Only cellular lengthening was observed in this case (Figure 10).

Generally, ciprofloxacin kills microbes by interfering with bacterial DNA replication and transcription through inhibition of DNA gyrase/topoisomerase II and DNA topoisomerase IV.[64] This eventually leads to the formation of quinolone-enzyme−DNA complexes and thus the generation of reactive oxygen species (ROS) with subsequent cellular death.[60] However, release of "active fragments" most probably did not affect the DNA replication, but rather, the enzymes of the SEDS family involved in septum formation were being mostly

DOI: 10.1021/acs.bioconjchem.8b00846
Bioconjugate Chem. 2019, 30, 218−230

affected. The final step of septum formation resulting in the formation of two daughter cells from one mother cell appears to be inhibited by this polymer. Again, DAPI staining indicated no change in the nucleic acid contents of the cells (Figure S16). This polymer might be affecting only the final stage of cell division as observed from chain formation. It could also inhibit the cells to proceed beyond G0 cell cycle stage as indicated by similar DAPI intensities in the cells. Increase in cell size could be indicative of stress resulting from low nutrient uptake in the presence of the polymer. Arrest at G0 could allow the cells to undertake necessary repairing to progress into cell cycle. This could result from the bacteriostatic activity observed in the liquid matrix.

CONCLUSIONS

In summary, a ciprofloxacin antibiotic appended zwitterionic polymeric hydrogel was developed where the antibiotic was conjugated to the polymer via ester linkage leading to generation of an efficient PAC structure. Matrix-dependent antibacterial activity was studied in the presence of our PACs against the novel bacterium *V. chemaguriensis* Iso1 strain. Sustained release of bioactive ciprofloxacin fragment from the gel showed antimicrobial activity in both solid and liquid matrices. Additionally, a forceful contact between the bacterial cell wall and active gel surface could only happen in solid matrix leading to complete growth inhibition and bactericidal effect with rod to sphere morphological transformation followed by chain formation with intact cell wall as a consequence of the "dual" mechanism. In the liquid matrix, an additional very thick EPS-like layer is produced by the bacterium upon treatment with the polymer and clearly visible in the TEM, which inhibits the bactericidal effect of our gel to a considerable extent. However, the growth was much lower compared with the control and linear analogous PACs. Hence, there was an enhancement of surface area in the studied bacterial cells without affecting the procular bodies and cell morphology. This further established matrix-assisted inhibition of antibacterial gel which is challenging. Interestingly this phenomenon is observed in some selective biofilm forming pathogenic bacterial strains such as the novel *V. chemaguriensis*. Thus, matrix-assisted inhibition of bacterial killing efficacy restricted the efficient bioapplications of our gel only in semisolid or solid matrix like the antibacterial coating of a pacemaker, artificial respiratory system, and so on.[65] Hence, future work should be dedicated to additional optimization of this kind of PAC, to disintegrate EPS layer generated in liquid matrix promoting contact-active killing efficacy, which could ultimately pave the way for new generation of antimicrobial therapeutics.

EXPERIMENTAL SECTION

Materials, instrumentations, synthesis of SBMA, different CTAs (Scheme S1), different architecture variable polymers and gel, measurement of swelling and deswelling kinetics, specific experimental procedure for antibacterial activity study in solid agar plate and liquid LB medium with corresponding morphology study via FESEM, TEM, and staining process are discussed in Supporting Information.

ASSOCIATED CONTENT

Supporting Information

The Supporting Information is available free of charge on the ACS Publications website at DOI: 10.1021/acs.bioconjchem.8b00846.

Synthetic scheme and characterization of Boc ciprofloxacin, Boc-cipro BBHT and Boc-cipro VBHT CTAs by NMR and ESI-MS; ZOI experiment against several bacteria, quantitative values of ZOI, growth experiment in LB medium, optical and epifluorescence microscopy images of stained pathogenic *V. chemaguriensis* cells under time-dependent treated condition (PDF)

AUTHOR INFORMATION

Corresponding Authors

*E-mail: p_de@iiserkol.ac.in.
*E-mail: pbhadury@iiserkol.ac.in.

ORCID

Anwesha Ghosh: 0000-0003-1765-9832
Priyadarsi De: 0000-0001-5486-3395

Notes

The authors declare no competing financial interest.

ACKNOWLEDGMENTS

Ishita Mukherjee acknowledges Council of Scientific and Industrial Research (CSIR), Government of India, for her senior research fellowship.

ABBREVIATIONS

V. chemaguriensis, *Vibrio chemaguriensis* Iso1; PEGMA, polyethylene glycol methyl ether methacrylate;; SBMA, zwitterionic sulphabetaine methacrylate; PACs, polymer antibiotic conjugates; EPS, exopolysaccharide; PNIPAM, poly(*N*-isopropylacrylamide); 3D, three-dimensional; AMPs, antimicrobial peptides; *V. alginolyticus*, *Vibrio alginolyticus*; *E. coli*, *Escherichia coli* XL10; *S. aureus*, *Staphylococcus aureus*; RAFT, reversible addition−fragmentation chain transfer; AIBN, 2,2′-azobis(isobutyronitrile); CTAs, chain transfer agents; Boc-cipro BBHT, *tert*-butyl carbamate(Boc)-ciprofloxacin *S*-benzyl *S*′-hydroxyethylthiocarbonate; Boc-cipro VBHT, Boc-ciprofloxacin *S*-(4-vinyl)benzyl *S*′′-hydroxyethylthiocarbonate; DCC, dicyclohexylcarbodiimide; DMAP, 4-(dimethylamino)-pyridine; ESI-MS, electrospray ionization mass spectrometry; $M_{n,theo}$, theoretical molecular weight; MW, molecular weight; DCM, dichloromethane; $CHCl_3$, chloroform; SR, swelling ratio; ZOI, zone of inhibition; LB, Luria broth; shape; TEM, transmission electron microscopy; SEDS, elongation, division and sporulation; F143, fluorescein-5-isothiocyanate; DAPI, 4′,6-diamidino-2-phenylindole; FESEM, field emission-scanning electron microscopy; ROS, reactive oxygen species.

REFERENCES

(1) Nimmagadda, A., Liu, X., Teng, P., Su, M., Li, Y., Qiao, Q., Khadka, N. K., Sun, X., Pan, J., Xu, H., Li, Q., and Cai, J. (2017) Polycarbonates with potent and selective antimicrobial activity toward gram-positive bacteria. *Biomacromolecules 18*, 87−95.

(2) Palermo, E. F., and Kuroda, K. (2009) Chemical structure of cationic groups in amphiphilic polymethacrylates modulates the antimicrobial and hemolytic activities. *Biomacromolecules 10*, 1416−1428.

(3) Owens, C. D., and Stoessel, K. (2008) Surgical site infections: epidemiology, microbiology and prevention. *J. Hosp. Infect. 70*, 3−10.

DOI: 10.1021/acs.bioconjchem.8b00846
Bioconjugate Chem. 2019, 30, 218−230

(4) Darley, E. S. R., and MacGowan, A. P. (2004) Antibiotic treatment of gram-positive bone and joint infections. *J. Antimicrob. Chemother. 53*, 928−935.
(5) Campoccia, D., Montanaro, L., and Arciola, C. R. (2006) The significance of infection related to orthopedic devices and issues of antibiotic resistance. *Biomaterials 27*, 2331−2339.
(6) Boucher, H. W., Talbot, G. H., Bradley, J. S., Edwards, J. E., Gilbert, D., Rice, L. B., Scheld, M., Spellberg, B., and Bartlett, J. (2009) Bad bugs, no drugs: no eskape! an update from the infectious diseases society of america. *Clin. Infect. Dis. 48*, 1−12.
(7) Spellberg, B., Powers, J. H., Brass, E. P., Miller, L. G., and Edwards, J. J. E. (2004) Trends in antimicrobial drug development: implications for the future. *Clin. Infect. Dis. 38*, 1279−1286.
(8) Vila, J., Sánchez-Céspedes, J., Sierra, J. M., Piqueras, M., Nicolás, E., Freixas, J., and Giralt, E. (2006) Antibacterial evaluation of a collection of norfloxacin and ciprofloxacin derivatives against multiresistant bacteria. *Int. J. Antimicrob. Agents 28*, 19−24.
(9) Craig, W. A. (2004) Overview of newer antimicrobial formulations for overcoming pneumococcal resistance. *Am. J. Med. Supplements 117*, 16−22.
(10) López-Cebral, R., Romero-Caamaño, V., Seijo, B., Alvarez-Lorenzo, C., Martín-Pastor, M., Concheiro, A., Landin, M., and Sanchez, A. (2014) Spermidine cross-linked hydrogels as a controlled release biomimetic approach for cloxacillin. *Mol. Pharmaceutics 11*, 2358−2371.
(11) Ghosh, S., Chakraborty, P., Saha, P., Acharya, S., and Ray, M. (2014) Polymer based nanoformulation of methylglyoxal as an antimicrobial agent: efficacy against resistant bacteria. *RSC Adv. 4*, 23251−23261.
(12) Duncan, R., Gac-Breton, S., Keane, R., Musila, R., Sat, Y. N., Satchi, R., and Searle, F. (2001) Polymer−drug conjugates, pdept and pelt: basic principles for design and transfer from the laboratory to clinic. *J. Controlled Release 74*, 135−146.
(13) Hoste, K., De Winne, K., and Schacht, E. (2004) Polymeric prodrugs. *Int. J. Pharm. 277*, 119−131.
(14) Zhao, Y.-J., Wei, W., Su, Z.-G., and Ma, G.-H. (2009) Poly (ethylene glycol) prodrug for anthracyclines via *n*-mannich base linker: design, synthesis and biological evaluation. *Int. J. Pharm. 379*, 90−99.
(15) Haag, R., and Kratz, F. (2006) Polymer therapeutics: concepts and applications. *Angew. Chem., Int. Ed. 45*, 1198−1215.
(16) Woo, G. L. Y., Yang, M. L., Yin, H. Q., Jaffer, F., Mittelman, M. W., and Santerre, J. P. (2002) Biological characterization of a novel biodegradable antimicrobial polymer synthesized with fluoroquinolones. *J. Biomed. Mater. Res. 59*, 35−45.
(17) Woo, G. L. Y., Mittelman, M. W., and Santerre, J. P. (2000) Synthesis and characterization of a novel biodegradable antimicrobial polymer. *Biomaterials 21*, 1235−1246.
(18) Pichavant, L., Bourget, C., Durrieu, M.-C., and Héroguez, V. (2011) Synthesis of pH-sensitive particles for local delivery of an antibiotic via dispersion ROMP. *Macromolecules 44*, 7879−7887.
(19) Parwe, S. P., Chaudhari, P. N., Mohite, K. K., Selukar, B. S., Nande, S. S., and Garnaik, B. (2014) Synthesis of ciprofloxacin-conjugated poly (L-lactic acid) polymer for nanofiber fabrication and antibacterial evaluation. *Int. J. Nanomed. 9*, 1463−1477.
(20) Ferguson, E. L., Azzopardi, E., Roberts, J. L., Walsh, T. R., and Thomas, D. W. (2014) Dextrin−colistin conjugates as a model bioresponsive treatment for multidrug resistant bacterial infections. *Mol. Pharmaceutics 11*, 4437−4447.
(21) Nathan, A., Zalipsky, S., Ertel, S. I., Agathos, S. N., Yarmush, M. L., and Kohn, J. (1993) Copolymers of lysine and polyethylene glycol: a new family of functionalized drug carriers. *Bioconjugate Chem. 4*, 54−62.
(22) Du, J., Bandara, H. M. H. N., Du, P., Huang, H., Hoang, K., Nguyen, D., Mogarala, S. V., and Smyth, H. D. C. (2015) Improved biofilm antimicrobial activity of polyethylene glycol conjugated tobramycin compared to tobramycin in pseudomonas aeruginosa biofilms. *Mol. Pharmaceutics 12*, 1544−1553.
(23) Lawson, M. C., Shoemaker, R., Hoth, K. B., Bowman, C. N., and Anseth, K. S. (2009) Polymerizable vancomycin derivatives for bactericidal biomaterial surface modification: structure−function evaluation. *Biomacromolecules 10*, 2221−2234.
(24) Turos, E., Shim, J.-Y., Wang, Y., Greenhalgh, K., Reddy, G. S. K., Dickey, S., and Lim, D. V. (2007) Antibiotic-conjugated polyacrylate nanoparticles: new opportunities for development of anti-MRSA agents. *Bioorg. Med. Chem. Lett. 17*, 53−56.
(25) Sarker, P., Shepherd, J., Swindells, K., Douglas, I., MacNeil, S., Swanson, L., and Rimmer, S. (2011) Highly branched polymers with polymyxin end groups responsive to pseudomonas aeruginosa. *Biomacromolecules 12*, 1−5.
(26) Hoque, J., and Haldar, J. (2017) Direct synthesis of dextran-based antibacterial hydrogels for extended release of biocides and eradication of topical biofilms. *ACS Appl. Mater. Interfaces 9*, 15975−15985.
(27) Konwar, A., Kalita, S., Kotoky, J., and Chowdhury, D. (2016) Chitosan-iron oxide coated graphene oxide nanocomposite hydrogel: a robust and soft antimicrobial biofilm. *ACS Appl. Mater. Interfaces 8*, 20625−20634.
(28) Li, P., Poon, Y. F., Li, W. F., Zhu, H. Y., Yeap, S. H., Cao, Y., Qi, X. B., Zhou, C. C., Lamrani, M., Beuerman, R. W., et al. (2011) A polycationic antimicrobial and biocompatible hydrogel with microbe membrane suctioning ability. *Nat. Mater. 10*, 149−156.
(29) Liu, S. Q., Yang, C., Huang, Y., Ding, X., Li, Y., Fan, W. M., Hedrick, J. L., and Yang, Y. Y. (2012) Antimicrobial and antifouling hydrogels formed in situ from polycarbonate and poly(ethylene glycol) via michael addition. *Adv. Mater. 24*, 6484−6489.
(30) Mi, L., Xue, H., Li, Y. T., and Jiang, S. Y. A. (2011) Thermoresponsive antimicrobial wound dressing hydrogel based on a cationic betaine ester. *Adv. Funct. Mater. 21*, 4028−4034.
(31) Zhou, C. C., Li, P., Qi, X. B., Sharif, A. R. M., Poon, Y. F., Cao, Y., Chang, M. W., Leong, S. S. J., and Chan-Park, M. B. (2011) A photopolymerized antimicrobial hydrogel coating derived from epsilon-poly-L-lysine. *Biomaterials 32*, 2704−2712.
(32) Li, Y., Fukushima, K., Coady, D. J., Engler, A. C., Liu, S. Q., Huang, Y., Cho, J. S., Guo, Y., Miller, L. S., Tan, J. P. K., et al. (2013) Broad-spectrum antimicrobial and biofilm-disrupting hydrogels: stereocomplex-driven supramolecular assemblies. *Angew. Chem., Int. Ed. 52*, 674−678.
(33) Lee, A. L. Z., Ng, V. W. L., Wang, W. X., Hedrick, J. L., and Yang, Y. Y. (2013) Block copolymer mixtures as antimicrobial hydrogels for biofilm eradication. *Biomaterials 34*, 10278−10286.
(34) Li, M., Mitra, D., Kang, E.-T., Lau, T., Chiong, E., and Neoh, K. G. (2017) Thiol-ol chemistry for grafting of natural polymers to form highly stable and efficacious antibacterial coatings. *ACS Appl. Mater. Interfaces 9*, 1847−1857.
(35) Shirbin, S. J., Lam, S. J., Chan, N. J.-A., Ozmen, M. M., Fu, Q., O'Brien-Simpson, N., Reynolds, E. C., and Qiao, G. G. (2016) Polypeptide-based macroporous cryogels with inherent antimicrobial properties: the importance of a macroporous structure. *ACS Macro Lett. 5*, 552−557.
(36) Hoque, J., Prakash, R. G., Paramanandham, K., Shome, B. R., and Haldar, J. (2017) Biocompatible injectable hydrogel with potent wound healing and antibacterial properties. *Mol. Pharmaceutics 14*, 1218−1230.
(37) Guo, J., Kim, G. B., Shan, D., Kim, J. P., Hu, J., Wang, W., Hamad, F. G., Qian, G., Rizk, E. B., and Yang, J. (2017) Click chemistry improved wet adhesion strength of mussel-inspired citrate-based antimicrobial bioadhesives. *Biomaterials 112*, 275−286.
(38) Hoque, J., Bhattacharjee, B., Prakash, R. G., Paramanandham, K., and Haldar, J. (2018) Dual function injectable hydrogel for controlled release of antibiotic and local antibacterial therapy. *Biomacromolecules 19*, 267−278.
(39) McMahon, S., Kennedy, R., Duffy, P., Vasquez, J. M., Wall, J. G., Tai, H., and Wang, W. (2016) Poly(ethylene glycol)-based hyperbranched polymer from RAFT and its application as a silver-sulfadiazine-loaded antibacterial hydrogel in wound care. *ACS Appl. Mater. Interfaces 8*, 26648−26656.

DOI: 10.1021/acs.bioconjchem.8b00846
Bioconjugate Chem. 2019, 30, 218−230

(40) Wu, F., Meng, G., He, J., Wu, Y., Wu, F., and Gu, Z. (2014) Antibiotic-loaded chitosan hydrogel with superior dual functions: antibacterial efficacy and osteoblastic cell responses. *ACS Appl. Mater. Interfaces 6*, 10005−10013.
(41) Lukaski, H. C., Bolonchuk, W. W., Hall, C. B., and Siders, W. A. (1986) Validation of tetrapolar bioelectrical impedance method to assess human body composition. *J. Appl. Physiol. 60*, 1327−1332.
(42) Gennari, M., Ghidini, V., Caburlotto, G., and Lleo, M. M. (2012) Virulence genes and pathogenicity islands in environmental Vibrio strains nonpathogenic to humans. *FEMS Microbiol. Ecol. 82*, 563−573.
(43) Timofeeva, L., and Kleshcheva, N. (2011) Antimicrobial polymers: mechanism of action, factors of activity, and applications. *Appl. Microbiol. Biotechnol. 89*, 475−492.
(44) Stewart, P. S., and William Costerton, J. (2001) Antibiotic resistance of bacteria in biofilms. *Lancet 358*, 135−138.
(45) Sellenet, P. H., Allison, B., Applegate, B. M., and Youngblood, J. P. (2007) Synergistic activity of hydrophilic modification in antibiotic polymers. *Biomacromolecules 8*, 19−23.
(46) Lalani, R., and Liu, L. (2012) Electrospun zwitterionic poly(sulfobetaine methacrylate) for nonadherent, superabsorbent and antimicrobial wound dressing applications. *Biomacromolecules 13*, 1853−1863.
(47) Kumar, S., Acharya, R., Chatterji, U., and De, P. (2013) Controlled synthesis of pH responsive cationic polymers containing side-chain peptide moieties via RAFT polymerization and their self-assembly. *J. Mater. Chem. B 1*, 946−957.
(48) Ulijn, R. V., and Smith, A. M. (2008) Designing peptide based nanomaterials. *Chem. Soc. Rev. 37*, 664−675.
(49) Roy, S. G., Haldar, U., and De, P. (2014) Remarkable swelling capability of amino acid based cross-linked polymer networks in organic and aqueous medium. *ACS Appl. Mater. Interfaces 6*, 4233−4241.
(50) Roy, S. G., and De, P. (2014) Swelling properties of amino acid containing cross-linked polymeric organogels and their respective polyelectrolytic hydrogels with pH and salt responsive property. *Polymer 55*, 5425−5434.
(51) Dong, R., Pang, Y., Su, Y., and Zhu, X. (2015) Supramolecular hydrogels: synthesis, properties and their biomedical applications. *Biomater. Sci. 3*, 937−954.
(52) Hu, B., Owh, C., Chee, P. L., Leow, W. R., Liu, X., Wu, Y.-L., Guo, P., Loh, X. J., and Chen, X. (2018) Supramolecular hydrogels for antimicrobial therapy. *Chem. Soc. Rev. 47*, 6917−6929.
(53) Cazedey, E. C. L., and Salgado, H. R. N. (2012) Spectrophotometric determination of ciprofloxacin hydrochloride in ophthalmic solution. *Adv. Analyt. Chem. 2*, 74−79.
(54) Li, M., De, P., Gondi, S. R., and Sumerlin, B. S. (2008) End group transformations of RAFT-generated polymers with bismaleimides: functional telechelics and modular block copolymers. *J. Polym. Sci., Part A: Polym. Chem. 46*, 5093−5100.
(55) Jagur-Grodzinski, J. (2010) Polymeric gels and hydrogels for biomedical and pharmaceutical applications. *Polym. Adv. Technol. 21*, 27−47.
(56) Bhattarai, N., Gunn, J., and Zhang, M. (2010) Chitosan-based hydrogels for controlled, localized drug delivery. *Adv. Drug Delivery Rev. 62*, 83−99.
(57) Mukherjee, I., Ghosh, A., Bhadury, P., and De, P. (2018) Leucine-based polymer architecture-induced antimicrobial properties and bacterial cell morphology switching. *ACS Omega 3*, 769−780.
(58) Tiller, J. C., Liao, C.-J., Lewis, K., and Klibanov, A. M. (2001) Designing surfaces that kill bacteria on contact. *Proc. Natl. Acad. Sci. U. S. A. 98*, 5981−5985.
(59) Dalgaard, P., Ross, T., Kamperman, L., Neumeyer, K., and McMeekin, T. A. (1994) Estimation of bacterial growth rates from turbidimetric and viable count data. *Int. J. Food Microbiol. 23*, 391−404.
(60) Masadeh, M., Alzoubi, K., Al-azzam, S., Khabour, O., and Al-buhairan, A. (2016) Ciprofloxacin-induced antibacterial activity is atteneuated by pretreatment with antioxidant agents. *Pathogens 5* (1−8), 28.
(61) Plemel, J. R., Caprariello, A. V., Keough, M. B., Henry, T. J., Tsutsui, S., Chu, T. H., Schenk, G. J., Klaver, R., Yong, V. W., and Stys, P. K. (2017) Unique spectral signatures of the nucleic acid dye acridine orange can distinguish cell death by apoptosis and necroptosis. *J. Cell Biol. 216*, 1163−1181.
(62) Franci, G., Falanga, A., Galdiero, S., Palomba, L., Rai, M., Morelli, G., and Galdiero, M. (2015) Silver nanoparticles as potential antibacterial agents. *Molecules 20*, 8856.
(63) Heinrich, K., Leslie, D. J., and Jonas, K. (2015) Modulation of bacterial proliferation as a survival strategy. *Adv. Appl. Microbiol. 92*, 127−171.
(64) Oliphant, C. M., and Green, G. M. (2002) Quinolones: a comprehensive review. *Am. Fam. Physician 65*, 455−464.
(65) Veerachamy, S., Yarlagadda, T., Manivasagam, G., and Yarlagadda, P. K. (2014) Bacterial adherence and biofilm formation on medical implants: a review. *Proc. Inst. Mech. Eng., Part H 228*, 1083−1099.

DOI: 10.1021/acs.bioconjchem.8b00846
Bioconjugate Chem. 2019, 30, 218−230